Eur. Phys. J. Appl. Phys. (2013) 64: 24510
DOI: 10.1051/epjap/2013120440

THE EUROPEAN PHYSICAL JOURNAL APPLIED PHYSICS

Regular Article

Efficient FEM modeling of printed coils for eddy current testing*

Houda Zaidi[1,2,a], Laurent Santandrea[1], Guillaume Krebs[1], Yann Le Bihan[1], and Edouard Demaldent[2]

[1] Laboratoire de Génie Electrique de Paris – UMR 8507 CNRS – Supelec – Univ. Paris-Sud and UPMC Plateau de Moulon, 91192 Gif-sur-Yvette Cedex, France
[2] CEA, LIST, 91191 Gif-sur-Yvette Cedex, France

Received: 2 October 2012 / Received in final form: 16 January 2013 / Accepted: 2 April 2013
Published online: 8 November 2013 –

Abstract. In this paper an approach for the modeling of the eddy current testing of a conductive part with flat printed coils is proposed. The overlapping finite element method is implemented for this purpose. It is shown that this approach allows simplifying the modeling of eddy current testing configurations that use this kind of coil.

1 Introduction

Eddy current testing (ECT) is a widely used technique for the inspection of conductive parts. It consists in scanning the part under investigation with a coil fed by a time-harmonic source current and to sense the response of the part with the same coil or with another one. A new trend in ECT lies in the use of printed coils obtained either by conventional printed circuit board technologies or by micro-technological processes [1,2]. This kind of coil used as transmitter and/or receiver exhibits several advantages. Indeed, the fabrication processes allow a good reproducibility of the coil physical characteristics and a miniaturization of the coils permits to design integrated multi-coil systems on a single substrate. Furthermore a good magnetic coupling can be obtained thanks to the possible reduction of the lift-off (the distance that separates the coil turns from the conductive part under inspection).

The finite element method (FEM) is well appreciated for its versatility. Nevertheless the modeling of an ECT configuration using printed coils is delicate since these coils are typically very flat with a diameter-to-height ratio which can reach the hundred. The meshing of thin coils with simplex elements (tetrahedra for a 3D problem) can then lead to a mesh containing a high number of elements or having deformed elements. It follows that the inversion of the FEM system will be time-consuming with possibly a poor solution.

In this paper the authors present a FEM approach that yields an efficiency taking into account of the presence of a flat probe. For this purpose the overlapping element method [3] is used. This method allows to model thin geometrical domains without degrading the mesh quality. Moreover the coil displacement can be taken into account without remeshing thanks to a non-conformal mesh connection. Overlapping method was used in reference [3] to take into account an air-gap domain and in reference [4] to consider thin material regions (magnetic and/or conductive). The originality of this paper lies in the introduction of a source current density term into the overlapping layer in order to take into account thin active regions (flat printed coils).

In what follows the implemented dual formulations and the overlapping element method are firstly presented. Then, two test cases are studied. The first test case is used to study and discuss the range of validity of our flat coil model. The second is an ECT configuration where the probe consists of two flat coils. The results are compared to reference models to show the applicability of the proposed technique.

2 Formulations

The use of dual FEM formulations is proposed in this paper to model ECT configurations. One formulation is deduced from the magnetic field $\boldsymbol{h}$ and the other one from the electrical field $\boldsymbol{e}$ [5]. The variables of work of the two formulations can be either the field (magnetic or electric) or combined vector-scalar potentials describing the field [5]. The use of these potentials is recommended in order to have more accurate results and better conditioned system [6]. As a consequence in this paper the formulations are expressed using combined vector and scalar potentials.

The first formulation, called $\boldsymbol{t}$-ϕ formulation, is based on a magnetic scalar potential ϕ and an electric vector potential $\boldsymbol{t}$ decomposition of the magnetic field:

$$\boldsymbol{h} = \boldsymbol{t} + \boldsymbol{t_0} - \mathbf{grad}(\boldsymbol{\phi}), \tag{1}$$

* Contribution to the Topical Issue "Numelec 2012", Edited by Adel Razek.

[a] e-mail: houda.zaidi@lgep.supelec.fr

with $\boldsymbol{t}$ and $\boldsymbol{t_0}$ introduced such as $\mathbf{curl}(\boldsymbol{t}) = \boldsymbol{j_i}$ and $\mathbf{curl}(\boldsymbol{t_0}) = \boldsymbol{j_0}$ where $\boldsymbol{j_i}$ and $\boldsymbol{j_0}$ are the induced current density in the conductive part and the source current density in the coil.

An electric scalar potential ψ and a magnetic vector potential $\boldsymbol{a}$ are used for the second formulation (called $\boldsymbol{a}$-ψ formulation) and lead to the following expression of the electric field:

$$\boldsymbol{e} = -\partial_t(\boldsymbol{a} + \mathbf{grad}(\boldsymbol{\psi})), \tag{2}$$

with $\mathbf{curl}(\boldsymbol{a}) = \boldsymbol{b}$, where $\boldsymbol{b}$ is the magnetic flux density.

3 Flat coil modeling

The overlapping finite element method consists in modeling a non-meshed gap D_0 located between two independent meshes D_1 and D_2 (Fig. 1a). This domain can have any physical property (air, conductive and/or magnetic medium [4]). In this paper D_0 contains the flat probe. Typically D_1 will consist in air and D_2 in the conductive part. The first step of the method consists in the detection of the interface surfaces between D_1 and D_0 and between D_2 and D_0. In the studied case, theses surfaces are denoted S_1 and S_2 (Fig 1b). In a 3D case, S_1 and S_2 are two surfaces meshed with triangular elements. Either S_1 or S_2 has to contain a 2D mask of the coil (surfacic mesh of the coil) (Fig. 1b). The two surfacic meshes (S_1 and S_2) may be different.

The steps for the coil modeling are presented in what follows. Firstly, the nodes of the surfaces S_1 and S_2 are projected, according to the z vertical axis on a plane located in D_0 (see Fig. 2a). Figure 2b represents an enlarged portion of the projection of S_1 and S_2 which generally gives polygonal intersections. In a second step, all the intersections between the triangles (mesh) of S_1 and S_2 are identified. Each non-triangular intersection is divided into triangles as shown in Figure 2b. Finally, the resulting nodes of the intersections are projected on S_1 and S_2. Each triangle issued from the intersection of the surfaces S_1 and S_2 leads, taking into account the thickness of D_0, to a prism. At the end of this procedure a prismatic mesh is built in D_0 (Fig. 2c). The set of prisms located under the mask represents the discretized coil (the other prisms consisting in an air domain). For each prism, a scalar function such as, ψ or ϕ, is interpolated with the shape functions of the six nodes of the two triangles from which the prism derives. By comparison, a vectorial function with tangential continuity, such as $\boldsymbol{a}$ or $\boldsymbol{t}$, is interpolated by the six shape functions of the edges of the two triangles plus the three shape functions of the vertical edges of the prism.

A reference element is implemented to calculate the integral terms of the FEM system over D_0. This last is illustrated in Figure 3. The overlapping method permits to connect arbitrary surfaces. Indeed, the triangles T_1 and T_2 can form two non-parallel planes. Figure 3 represents the reference element (Fig. 3a) and the actual element (Fig. 3b). This latter is constituted by an integration area (prism), P, and by two triangles (T_1 and T_2) from which the area derives. A geometric transformation F_K is defined as:

$$F_K : \hat{P} \to P \quad \text{with} \quad F_K(\hat{x}, \hat{y}, \hat{z}) = \langle N(\hat{x}, \hat{y}, \hat{z}) \rangle T \tag{3}$$

and T expressed as:

$$T = \begin{pmatrix} x_1 & y_1 & z_1 \\ x_2 & y_2 & z_2 \\ x_3 & y_3 & z_3 \\ x_4 & y_4 & z_4 \\ x_5 & y_5 & z_5 \\ x_6 & y_6 & z_6 \end{pmatrix} \tag{4}$$

and N as:

$$\langle N(\hat{x}, \hat{y}, \hat{z}) \rangle = \langle \hat{\lambda}_1(\hat{x}, \hat{y}, \hat{z}), \hat{\lambda}_2(\hat{x}, \hat{y}, \hat{z}), \\ \hat{\lambda}_3(\hat{x}, \hat{y}, \hat{z}), \hat{\lambda}_4(\hat{x}, \hat{y}, \hat{z}), \hat{\lambda}_5(\hat{x}, \hat{y}, \hat{z}), \hat{\lambda}_6(\hat{x}, \hat{y}, \hat{z}) \rangle \tag{5}$$

where $(x_1, y_1, z_1), (x_2, y_2, z_2), \ldots, (x_6, y_6, z_6)$ are the coordinates of the nodes associated with the overlapping element K (i.e., the coordinates of $N_1, N_2, \ldots, N_6$) and

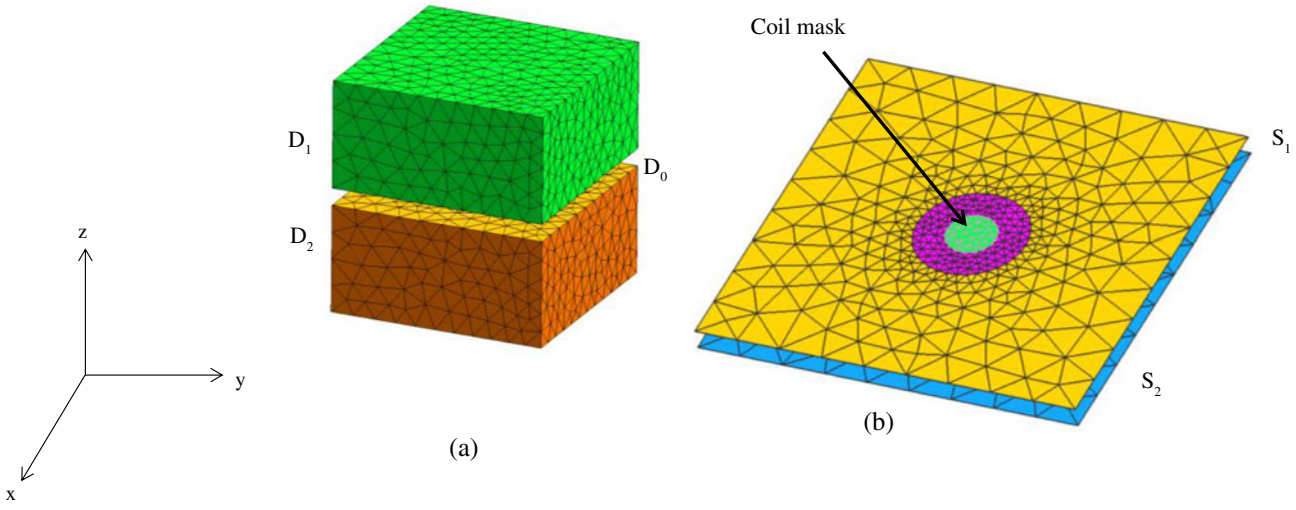

Fig. 1. (a) Test configuration in 3D, (b) surfaces to connect.

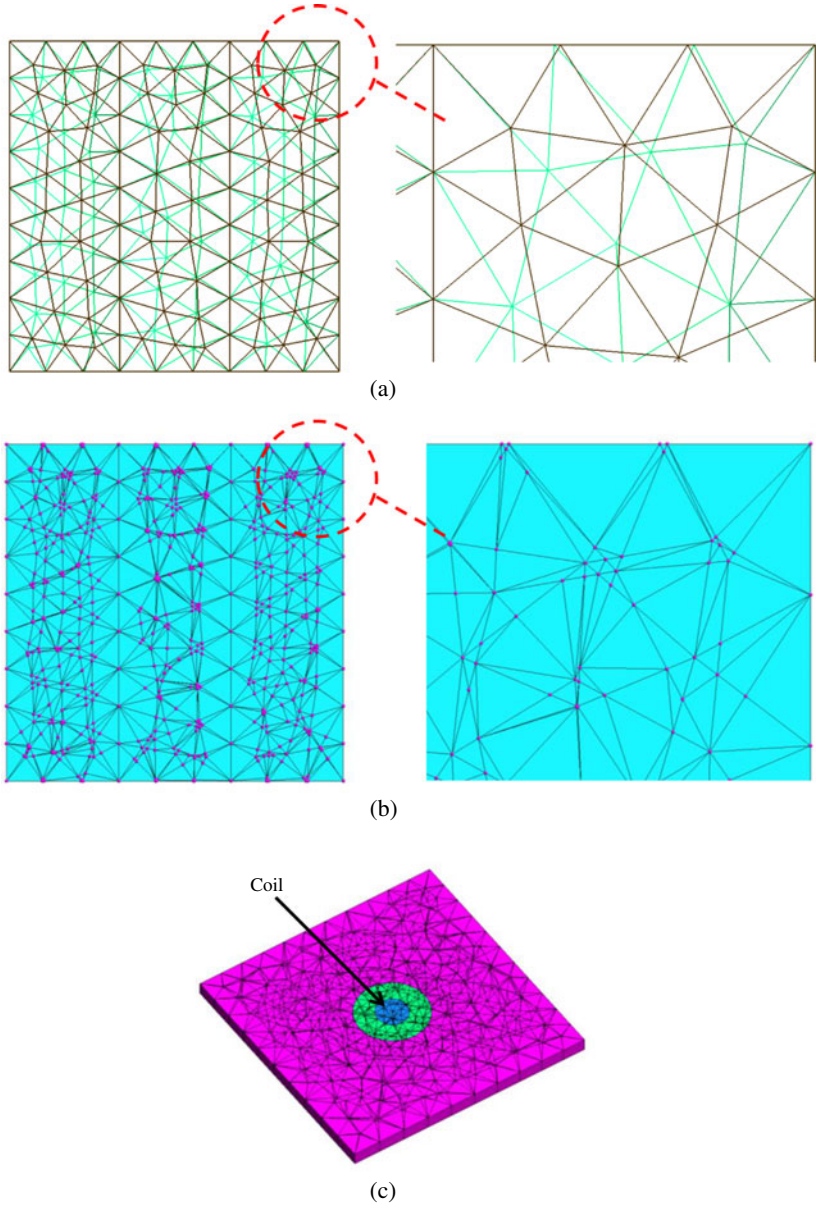

Fig. 2. (a) Projection of S_1 and S_2 on the same plane, (b) intersections of the triangles of S_1 and S_2, (c) subdivision of D_0 into prisms.

$\hat{\lambda}_1(\hat{\lambda}_2, \ldots, \hat{\lambda}_6$ respectively) is the nodal shape function associated to $\hat{N}_1(\hat{N}_2, \ldots, \hat{N}_6$ respectively) in the reference element. The coordinates $(a_i, b_i, \pm 1), i \in \{1, \ldots, 6\}$ are calculated for each integration area by solving the following simple system:

$$F_{\mathrm{K}}(\hat{P}) = P. \tag{6}$$

The six shape functions [7] associated to the nodes $\hat{N}_{\mathrm{i}}$, $i \in \{1, \ldots, 6\}$ can be expressed as follows:

$$\begin{cases} \hat{\lambda}_i(\hat{x}, \hat{y}, \hat{z}) = \dfrac{1-\hat{z}}{2} \hat{\lambda}_i^{\hat{T}_1}(\hat{x}, \hat{y}) \quad i \in \{1, 2, 4\} \\ \hat{\lambda}_i(\hat{x}, \hat{y}, \hat{z}) = \dfrac{1+\hat{z}}{2} \hat{\lambda}_{i-3}^{\hat{T}_2}(\hat{x}, \hat{y}) \; i \in \{4, 5, 6\} \end{cases}, \tag{7}$$

where $\hat{\lambda}_i^{\hat{T}_1}(\hat{x}, \hat{y})$, $i \in \{1, 2, 3\}$ ($\hat{\lambda}_i^{\hat{T}_2}(\hat{x}, \hat{y})$, $i \in \{1, 2, 3\}$, respectively) are the three nodal shape functions associated to the triangle $\hat{T}_1$ ($\hat{T}_2$, respectively). The two weighting $\frac{1+/-\hat{z}}{2}$ are used to extend these 2D shape functions and insuring the continuity of the interpolated scalar field in D_0 and on its interfaces.

The nodal shape functions are associated to the two triangles from which the prism derives. It follows that the influence of the domain D_0 on the conditioning of the matrix system and on the convergence and accuracy of the system solver only depends on the quality of the initial S_1 and S_2 triangular meshes.

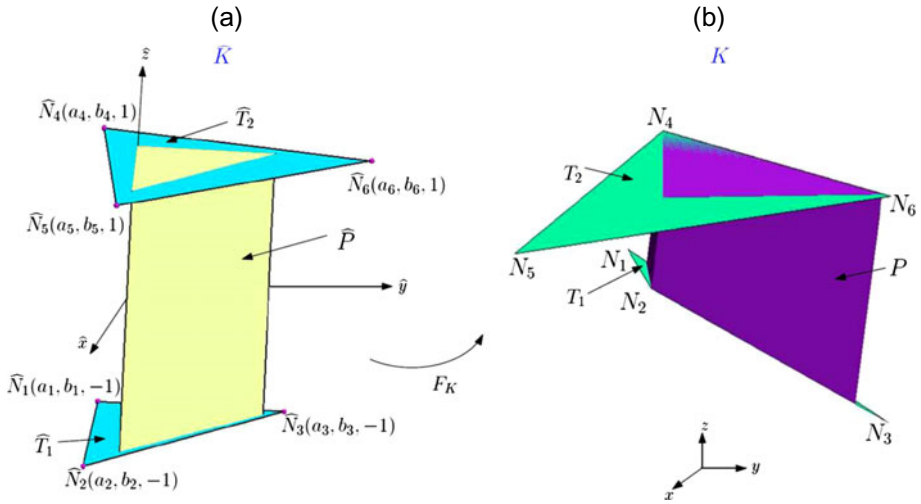

Fig. 3. Reference element used for the calculation of the integral terms.

Table 1. Parameters of the first test case.

Coil inner radius (mm)	0.53
Coil outer radius (mm)	11.05
Number of coil turns	70
Excitation frequency (kHz)	1

The edge shape function expressions are:

$$\begin{cases} \hat{\psi}_i(\hat{x},\hat{y},\hat{z}) = \dfrac{1-\hat{z}}{2}\hat{\psi}_i^{\hat{T}_1}(\hat{x},\hat{y}) \quad i \in \{1,2,3\} \\ \hat{\psi}_i(\hat{x},\hat{y},\hat{z}) = \hat{\psi}_i^{\hat{P}}(\hat{x},\hat{y},\hat{z}) \quad i \in \{4,5,6\} \\ \hat{\psi}_i(\hat{x},\hat{y},\hat{z}) = \dfrac{1+\hat{z}}{2}\hat{\psi}_{i-6}^{\hat{T}_2}(\hat{x},\hat{y}) \quad i \in \{7,8,9\} \end{cases} \tag{8}$$

where $\hat{\psi}_i^{\hat{T}_1}(\hat{x},\hat{y})\, i \in \{1,2,3\}$ ($\hat{\psi}_i^{\hat{T}_2}(\hat{x},\hat{y})\, i \in \{1,2,3\}$, respectively) are the three edge shape functions associated to the triangle $\hat{T}_1$ ($\hat{T}_2$, respectively) and $\hat{\psi}_i^{\hat{P}}(\hat{x},\hat{y},\hat{z})$ $i \in \{4,5,6\}$ are the edge shape functions associated to the three vertical edges of $\hat{P}$. These three last shape functions correspond to new edge unknowns introduced in the D_0 domain. For each prism six horizontal edges are considered and three vertical edges are added in the system of unknowns. The six horizontal edges are associated with two triangles (one issued from the S_1 mesh and the other from the S_2 mesh) then the influence of these edges on the conditioning of the matrix system and on the convergence and accuracy of the system solver only depends on the quality of the initial S_1 and S_2 triangular meshes. By cons, the three vertical edges are associated to the prism. These edges can become very small when considering a very thin domain. Nevertheless the prism can be flattened in some measure without significant increase of the conditioning of the matrix system. It follows that in practice conditioning problems were not encountered in this work.

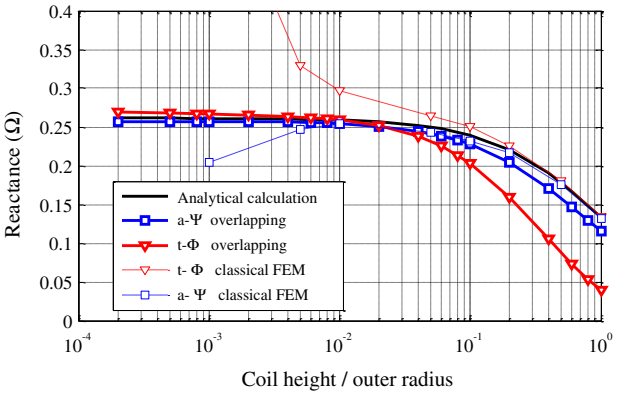

Fig. 5. Reactance of the coil vs. height/radius ratio.

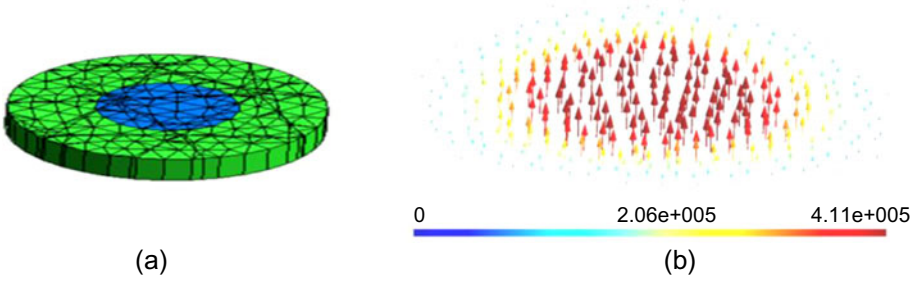

Fig. 4. (a) Prismatic mesh of the coil, (b) source vector $\boldsymbol{t}_0$ (A/m) calculated in each prism of the coil mesh.

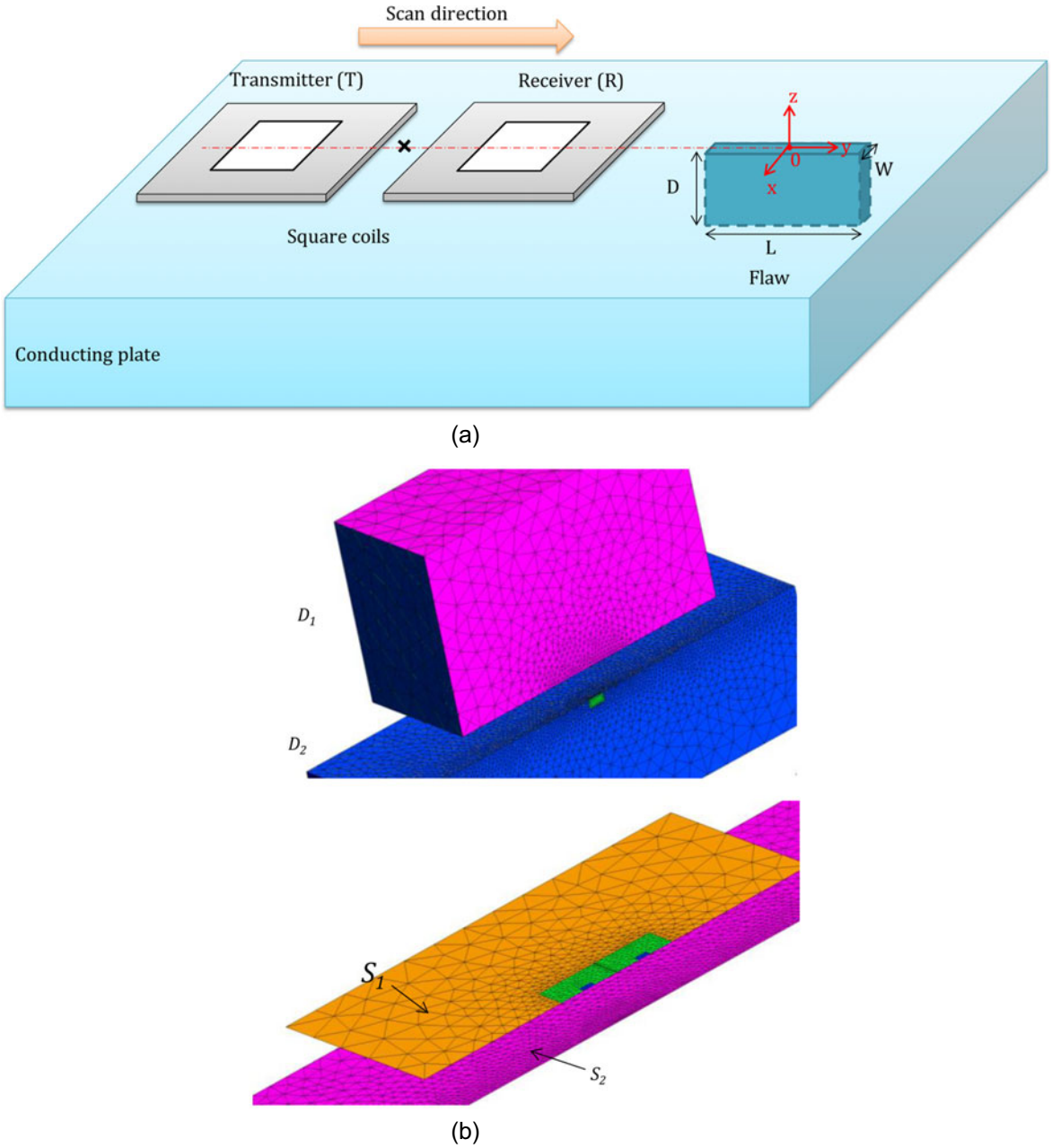

Fig. 6. (a) Description of the second test case, (b) mesh of the different subdomains.

The source vector potential $\boldsymbol{t_0}$ describing for both formulations the coil current density is non-null in the coil and in its (air or magnetic) internal core. It can be calculated analytically for a simple coil geometry or by FEM for complex coil configurations (e.g., distorted flexible coil) [8]. Since $\boldsymbol{t_0} \times \boldsymbol{n} = \boldsymbol{0}$ has to be verified on the boundary of the domain of $\boldsymbol{t_0}$ [5], $\boldsymbol{t_0}$ is discretized on the vertical edges of D_0 belonging to the coil and its core.

4 Tests and results

4.1 Flat coil in air

In this first example, the range of validity of the modeling of a flat coil with our method is evaluated. The source current density of the coil can be described either with an analytical or with a numerical approach depending on the geometrical complexity of the coil. In the example the coil is axisymmetrical as shown in its mesh of Figure 4a. In this study t_0 is calculated analytically. It is parallel to the coil axis and its distribution is shown in Figure 4b. Table 1 gives the parameters of the coil. The coil is placed in air. As usual in ECT modeling the coil is treated as a non-conducting domain crossed by a current density of uniform intensity [9]. Its apparent resistance is then null in the absence of conducting part since the resistance due to the coil wires is not considered in the modeling. The coil reactance has been calculated with respect to the coil height for the two formulations by the overlapping method and by the classical FEM with only tetrahedral

Table 2. Parameters of the second test case.

Coil parameters	
Length of the inner side (mm)	0.21
Length of the outer side (mm)	1
Number of turns	40
Height (μm)	20
Lift-off (μm)	50
Gap between the two coils (μm)	5
Frequency (MHz)	4
Flaw parameters	
Length L (mm)	0.4
Depth D (mm)	0.2
Width W (mm)	0.1
Plate parameters	
Conductivity (MS/m)	0.76
Thickness (mm)	3

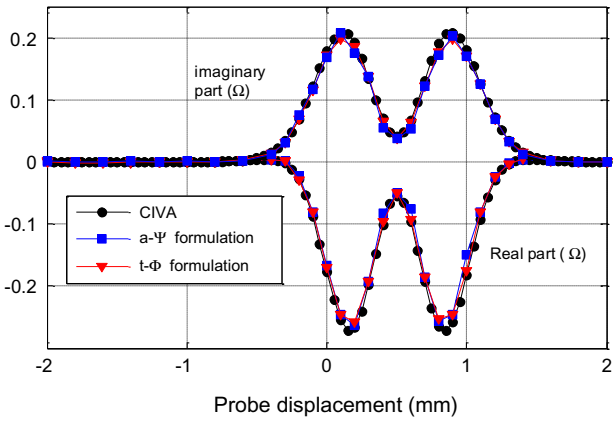

Fig. 7. Variation of the transmitter impedance due to the flaw.

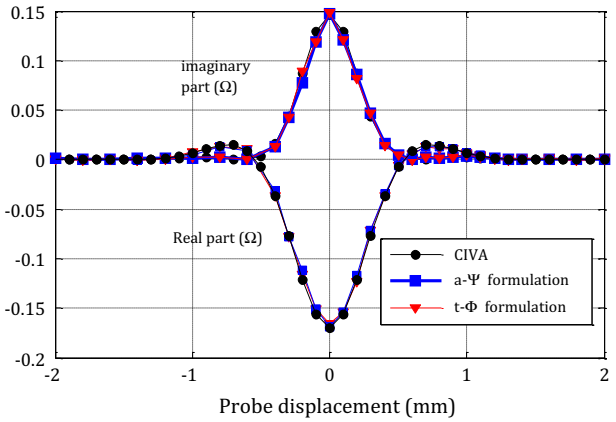

Fig. 8. Variation of the probe transimpedance due to the flaw.

elements. A comparison with an analytical magnetodynamic model [9] is also provided, see Figure 5. The two formulations with the overlapping method are very close to the analytical calculation for a height ranging until several percent of the outer radius. Above 10% of the outer radius, the mesh of the coil becomes too coarse since there is only one layer of overlapping element in this example. Nevertheless, the use of the overlapping method is unnecessary in this case since the classical FEM calculation becomes satisfactory. The number of elements of the classical FEM meshes varied between 27 550 tetrahedra for a very flat coil and 82 882 for the thickest one. The computation time rises for the coils with small thicknesses which may be due to the bad quality of some elements of the mesh. The number of elements of the mesh with the overlapping method is constant: 27 624 tetrahedra and 6274 prisms created in the overlapping domain.

4.2 Separated function probe with flat coils

In this test case, a probe with separated transmitter (T) and receiver (R) functions is considered. One coil (transmitter) is used to create an alternating electromagnetic field while a second coil (receiver) is used for the reception of the response of the tested material. This type of probe is usually more efficient than the double function probes (one coil acting simultaneously as transmitter and receiver) since it is generally less sensitive to external perturbations. The T-R probe is made of two identical rectangular flat coils and is moved along the length of a rectangular flaw present in a conductive plate. The configuration is illustrated in Figure 6a and its parameters are given in Table 2.

The studied domain is divided into two parts. The first part, D_1, is a box of air while the second part, D_2, contains the conducting plate (Fig. 6b). These two domains are separated by two non-meshed layers where overlapping elements are applied (once the integration areas are detected in D_0, a division of D_0 in several layers can be easily performed [4]). The top layer is for the probe and the other one for the lift-off domain (air). For the modeling of the probe, a 2D surface S_{12} is added between S_1 (which includes the 2D mask of the probe) and S_2. S_{12} is the duplication of S_1 between the two surface meshes S_1, S_2 in such a way that the thickness between S_{12} and S_1 is equal to the thickness of the coils whereas the thickness between S_{12} and S_2 is equal to the lift-off thickness. The probe is taken into account by the application of overlapping elements between S_1 and S_{12}. The lift-off is taken into account by applying the same technique between S_{12} and S_2.

The probe and the flaw are centered along the x axis (Fig. 6). The 1D scan along the flaw length is performed without remeshing by displacing the box D_1 and by applying the overlapping method for each probe position. For each of these positions, the impedance of the transmitting coil and the transimpedance of the probe are calculated. These calculations are performed for both electric and magnetic formulations. The real part of the impedance of the transmitting coil is determined by calculating the Joule losses in the conductive media. The imaginary part of this impedance is determined from the magnetic energy stored in the entire meshed space. The probe

transimpedance is defined as:

$$Z_{\mathrm{TR}} = \frac{j\omega\phi_{\mathrm{R}}}{I_{\mathrm{T}}}, \tag{9}$$

where ϕ_{R} is the magnetic flux generated in the receiving coil, I_{T} is the intensity of the current passing through the transmitting coil, $j = \sqrt{-1}$ and ω is the pulsation. The calculation of the flux is presented in reference [10], for both dual formulations. The variations of the impedance and of the transimpedance due to the flaw are calculated by subtracting for each of them the values with and without flaw.

As part of collaboration with the laboratory LIST from CEA, the FEM results are compared with results issued from the software CIVA [11]. This software developed at CEA is based on the volume integral method. Figure 7 shows the imaginary and real parts of the variation of the impedance of the transmitter coil during the scan. Figure 8 represents the imaginary and real parts of the variation of the probe transimpedance during the scan.

It can be observed that the results of the two FEM formulations are very close to the CIVA calculations. It can be concluded that the proposed approach is well adapted to model flat probes and their displacement.

5 Conclusion

In this paper, the overlapping method has been used for the modeling of flat printed coils used in ECT. The displacement of the probe is also taken into account with this method. From the two test cases the following conclusions are drawn. Firstly, this method provides a satisfactory approximation for the modeling of the printed coils. In fact, a large range of flat probes can be considered with this technique (e.g., double or separated function probes with circular or rectangular coils). Secondly, it is well suited to take into account the displacement of the probe without remeshing thanks to the non-conformal mesh connection of the method. Moreover, this technique is well adapted for modeling several kinds of thin layers with different physical characteristics. In this way the lift-off of the probe can be easily taken into account in the modeling by adding a second layer of overlapping elements.

This work was supported by DIGITEO, Île-de-France Region and CEA LIST.

References

1. C. Ravat, P.-Y. Joubert, Y. Le Bihan, C. Marchand, M. Woytasik, E. Dufour-Gergam, Sen. Lett. **7**, 400 (2009)
2. B. Marchand, J.M. Decitre, O. Casula, Prog. Quant. Nondestructive Eval. **29**, 385 (2010)
3. H. Zaidi, L. Santandréa, G. Krebs, Y. Le Bihan, E. Demaldent, IEEE Trans. Magn. **48**, 583 (2012)
4. H. Zaidi, L. Santandréa, G. Krebs, Y. Le Bihan, E. Demaldent, *International Symposium on Applied Electromagnetics and Mechanics (ISEM), Napoli, Italy, 2011*
5. Z. Ren, A. Razek, Int. J. Num. Model. Electron. Netw. Dev. Fields **9**, 81 (1996)
6. M. Bensetti, Y. Choua, L. Santandrea, Y. Le Bihan, C. Marchand, IEEE Trans. Magn. **44**, 1646 (2008)
7. Z. Ren, IEEE Trans. Magn. **34**, 2547 (1998)
8. I. Chang-Hwan, K. Hong-Kyu, J. Hyun-Kyo, IEEE Trans. Magn. **38**, 505 (2008)
9. C.V. Dodd, W.E. Deeds, J. Appl. Phys. **39**, 2829 (1967)
10. Y. Choua, L. Santandréa, Y. Le Bihan, C. Marchand, IEEE Trans. Magn. **46**, 2795 (2010)
11. G. Pichenot, C. Reboud, R. Raillon, S. Mahaut, Ann. Rev. Prog. QNDE Proc. 1975 (2007)
12. R.J. Ditchburn, S.K. Burke, M. Posada, J. Nondestructive Eval. **22**, 63 (2003)